

Understanding Age-Induced Cortical Porosity in Women: The Accumulation and Coalescence of Eroded Cavities Upon Existing Intracortical Canals Is the Main Contributor

Christina Møller Andreasen,^{1,2} Jean-Marie Delaisse,² Bram CJ van der Eerden,³ Johannes PTM van Leeuwen,³ Ming Ding,¹ and Thomas Levin Andersen²

¹Orthopaedic Research Laboratory, Department of Orthopaedic Surgery & Traumatology, Odense University Hospital, Department of Clinical Research, University of Southern Denmark, Odense, Denmark

²Department of Clinical Cell Biology, Vejle Hospital/Lillebaelt Hospital, Institute of Regional Health Research, University of Southern Denmark, Vejle, Denmark

³Laboratory for Calcium and Bone Metabolism, Department of Internal Medicine, Erasmus MC, Rotterdam, The Netherlands

ABSTRACT

Intracortical bone remodeling normally ensures maintenance of the cortical bone matrix and strength, but during aging, this remodeling generates excessive porosity. The mechanism behind the age-induced cortical porosity is poorly understood and addressed in the present study. This study consists of a histomorphometric analysis of sections of iliac bone specimens from 35 women (age 16–78 years). First, the study shows that the age-induced cortical porosity reflects an increased pore size rather than an increased pore density. Second, it establishes a novel histomorphometric classification of the pores, which is based on the characteristics of the remodeling sites to which each pore is associated. It takes into consideration (i) the stage of the remodeling event at the level where the pore is sectioned, (ii) whether the event corresponds with the generation of a new pore through penetrative tunneling (type 1 pores) or with remodeling of an existing pore (type 2 pores), and (iii) in the latter case, whether or not the new remodeling event leads to the coalescence of pores. Of note, the advantage of this classification is to relate porosity with its generation mechanism. Third, it demonstrates that aging and porosity are correlated with: a shift from type 1 to type 2 pores, reflecting that the remodeling of existing pores is higher; an accumulation of eroded type 2 pores, reflecting an extended resorption-reversal phase; and a coalescence of these eroded type 2 pores into enlarged coalescing type 2 cavities. Collectively, this study supports the notion, that age-related increase in cortical porosity is the result of intracortical remodeling sites upon existing pores, with an extended reversal-resorption phase (eroded type 2 pores) that may likely result in a delayed or absent initiation of the subsequent bone formation. © 2017 The Authors. *Journal of Bone and Mineral Research* Published by Wiley Periodicals Inc.

KEY WORDS: CORTICAL BONE; CORTICAL POROSITY; BONE REMODELING; BONE RESORPTION; BONE FORMATION; AGING; COUPLING

Introduction

Cortical bone has been investigated for more than 300 years^(1,2) and has been at the origin of our present perception of the bone remodeling process, establishing that bone resorption precedes bone formation.^(3,4) Still, very little is known about the critical events contributing to the loss of cortical bone during aging, causing an increased cortical porosity and a reduced cortical thickness.^(5–7) The increased cortical porosity is undoubtedly due to an age-related dysfunction in the intracortical bone remodeling process, which under

physiological conditions renews cortical bone matrix in order to maintain its mechanical properties throughout life.^(8,9) The nature of this dysfunction in the remodeling process remains still to be resolved.

The intracortical bone remodeling is often referred to as Haversian remodeling and classically depicted as a cutting cone with bone resorbing osteoclasts excavating a canal, which is refilled by the coupled closing cone with bone forming osteoblasts subsequently refilling the canal until only a narrow canal remains.^(9,10) A recent study has elaborated on the organization of the cutting cone, demonstrating that the initial

This is an open access article under the terms of the Creative Commons Attribution License, which permits use, distribution and reproduction in any medium, provided the original work is properly cited.

Received in original form August 17, 2017; revised form November 17, 2017; accepted November 27, 2017. Accepted manuscript online November 29, 2017.

Address correspondence to: Christina M Andreasen, PhD, Orthopaedic Research Laboratory, Department of Orthopaedic Surgery and Traumatology O, Odense University Hospital, J. B. Winsloewsvej 15, Ground floor, DK-5000 Odense C, Denmark. E-mail: cmandreasen@health.sdu.dk

Additional Supporting Information may be found in the online version of this article.

Journal of Bone and Mineral Research, Vol. 33, No. 4, April 2018, pp 606–620

DOI: 10.1002/jbmr.3354

© 2017 The Authors. *Journal of Bone and Mineral Research* Published by Wiley Periodicals, Inc.

penetrative resorption process carried out by densely packed osteoclasts is followed by secondary resorption conducted by scattered osteoclasts intermixed with osteoblastic reversal cells.⁽¹¹⁾ This so-called reversal-resorption phase widens the canal until bone formation is initiated.⁽¹¹⁾ This study further highlights that a delayed initiation of bone formation leads to an extended secondary resorption and hereby a wider resorption space.⁽¹¹⁾ The extent of the space resorbed by each remodeling event is delineated by its cement line, which is embedded in the bone matrix during subsequent bone formation. In cross-sections, the intracortical remodeling sites can be observed as eroded pores, when in the initial resorption phase or the reversal-resorption phase, or as formative or quiescent pores of osteons, when the bone formation was ongoing or terminated. In cross-sectioned osteons, the extent of area that underwent resorption is delineated by a cement line, on which the new bone is deposited.

Cancellous and cortical bone loss during aging and osteoporosis has often been depicted to be the results of an insufficient refilling of the resorbed cavities, due to premature termination of bone formation.^(12–19) Recent studies have, however, demonstrated that cancellous bone loss in osteoporotic patients and osteopenic animals may also be the result of delayed or absent initiation of bone formation, causing an accumulation of remodeling sites in the reversal-resorption phase,^(20–25) as earlier suggested by several authors.^(26–28) In cortical bone, the unanswered question is whether the reported increased cortical porosity during aging results from: (i) a delayed or absent initiation of bone formation as suggested by Parfitt⁽²⁷⁾; or (ii) the accumulation of enlarged quiescent pores of osteons, due to an insufficient bone formation refilling of the resorbed space, a so-called negative BMU balance^(19,29) as investigated by Melsen's group.^(12,14)

The present study is part of a larger effort to characterize the intracortical remodeling events contributing to increased cortical porosity during aging, in order to answer the latter highlighted question. A novel histological classification of the pores was designed, based on the characteristics of the remodeling events shown at the level of these pores. This includes the stage of the intracortical remodeling events at the level of the histological section; their remodeling type, because intracortical bone remodeling events may not only generate new canals, but also remodel preexisting canals, as sporadically reported a long time ago^(10,30–34) and recently illustrated using synchrotron radiation μ CT^(35,36); and their position relative to preexisting osteons. This classification integrates and embraces many of the separate categories reported in the literature,^(12,30–34,36–39) but which are purely descriptive. In contrast, the present classification has the advantage to relate porosity with its generation mechanism, thus automatically showing which biological characteristics contribute the most to age-induced cortical porosity. The present study focuses on the histological characteristics of the pores classified categories of intracortical remodeling sites, their prevalence, size, and contribution to the overall porosity and their association with age and cortical porosity in iliac bone specimens from women.

Materials and Methods

Human bone specimens and sectioning

The intracortical bone remodeling was analyzed using undecalcified methylmethacrylate-embedded iliac crest bone specimens taken

2 cm behind the left anterior superior spine from 35 women (aged 16–78 years) during a forensic examination due to a sudden unexpected death. None of the women showed any clinical evidence of metabolic bone diseases, nor received any drugs affecting the calcium metabolism, thus considered representative of a normal population.⁽⁶⁰⁾ Cross-sections, 7- μ m-thick, were cut, stained with Masson's trichrome,⁽⁴⁰⁾ and exposed to a detailed histomorphometric investigation. For the 3D-reconstruction, 80 consecutive 7- μ m-thick sections were cut from one iliac specimen. Every other section was stained with Masson's trichrome, while the remaining sections were immunostained for osteopontin.

The study was approved by the Medical Ethical Committee Erasmus MC (2016-391) in compliance with the World Medical Association Declaration of Helsinki–Ethical Principle for Medical Research Involving Human Subjects.

Immunostaining

The methylmethacrylate-embedding on the sections was first removed using a xylene/chloroform mixture and 2-methoxyethyl-acetate followed by rehydration and decalcification in 1% acetic acid. Afterward, the sections were blocked with 0.5% casein (Sigma-Aldrich, Copenhagen, Denmark) in Tris-buffered saline (TBS: 0.05M Tris-HCl [pH 7.6] + 0.15M NaCl) and an avidin/biotin blocking kit (DAKO, Glostrup, DK). The sections were immunostained with biotinylated goat anti-osteopontin antibodies (BAF1433; R&D Systems, Minneapolis, MN, USA)⁽¹¹⁾ diluted in Renoir Red (PD904; Biocare Medical, Concord, CA, USA), which were detected with alkaline phosphatase-conjugated streptavidin (016-050-084; Jackson ImmunoResearch, Suffolk, UK) and visualized with Liquid Permanent Red (DAKO, Glostrup, DK). Finally, the sections were counterstained with Mayer's hematoxylin and then mounted using Aquatex.

Histomorphometry

The analysis was performed on both cortices within a 6.5-mm-wide zone, starting 20 mm from the iliac crest, as depicted in Fig. 1A. The analysis was restricted to a 6.5-mm-wide zone, in order to have a sufficient, but manageable, number of pores per bone specimen (mean 117 pores per bone specimen; range, 63–179 pores), which was placed with the largest distance as possible to the less well defined cortex at the iliac crest. The border between cortical and trabecular bone was carefully outlined based on both the bones structure and the lamellae structure of the bone matrix (Fig. 1B); making it possible separate the hemi-osteonal remodeled trabecular bone from the osteonal remodeled cortical bone.⁽⁹⁾ The presence of marrow cells and adipocytes could not be used to guide the border between the cortical and trabecular bone, because their presence appeared primarily related to the size of the pores, even when deeply embedded in the cortex. Within this zone each pore/osteone, in total 4095, was given an identification number and marked onto a printed map of the cortices (Fig. 1B). By use of polarized light, the surrounding lamellae and cement lines were clearly visualized (Fig. 2). Based on the literature and the initial systematic histological investigation of the intracortical pores/osteons, we realized that it was appropriate to categorize the pores according to the characteristics of the remodeling sites to which these pores were associated. These characteristics included:

1. The remodeling type of the pores, either type 1 or type 2. Pores were defined as type 1 pores when associated with a resorptive area that had no overlap with the pore of an

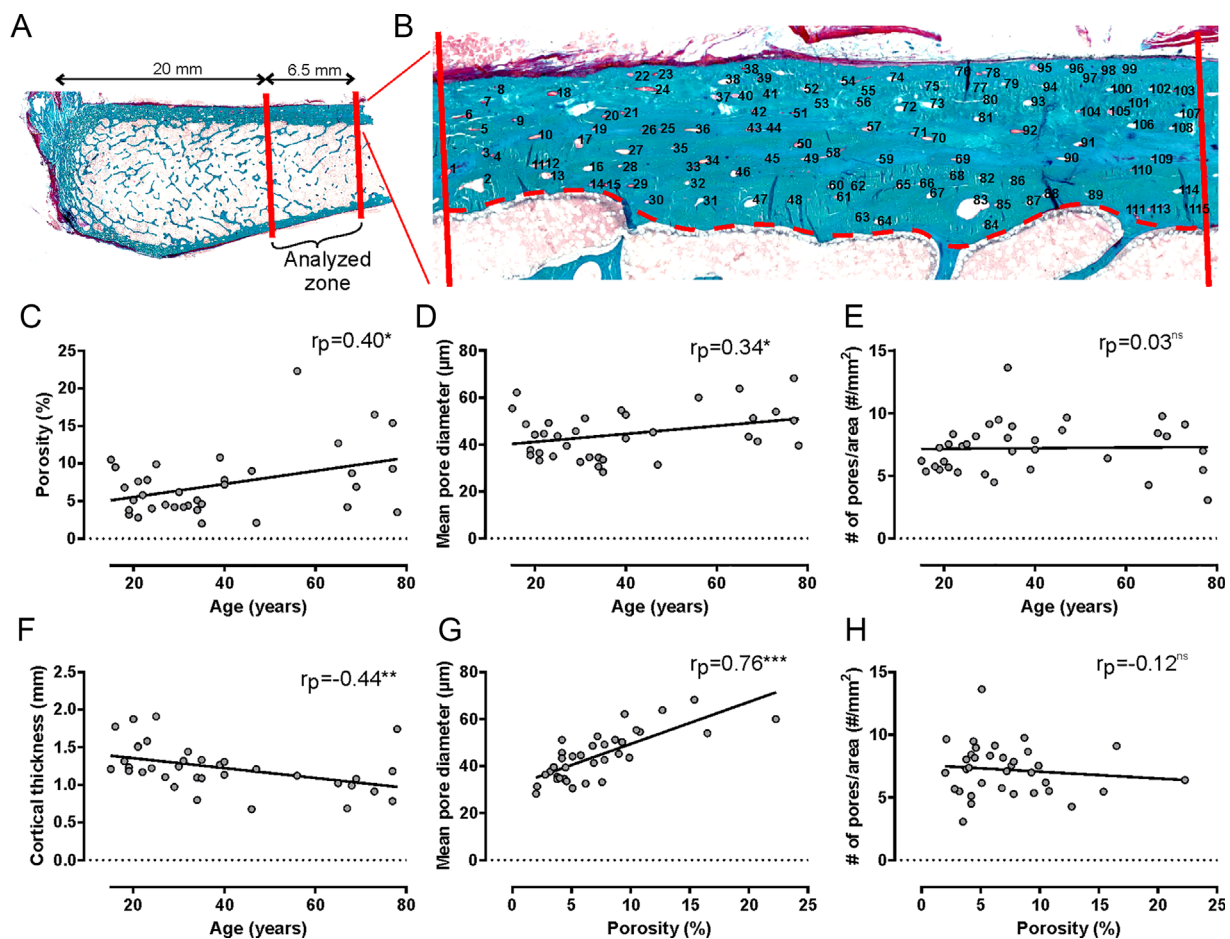


Fig. 1. General analysis of age-induced cortical porosity. (A) Both cortices of ilium bone specimens from 35 women were analyzed over the indicated zone of 6.5 mm starting 20 mm from the iliac crest. (B) Each pore and its associated remodeling site was identified, measured, classified and marked onto a map. The border between the cortical and trabecular bone is marked with a hatched line. (C–H) The cortical porosity (C) and mean pore diameter (D) were positively correlated with age, the number of pores/area was not correlated with age (E), and the cortical thickness was negatively correlated with age (F). The cortical thickness is the mean thickness of the inner and outer cortices together. The mean pore diameter was positively correlated with porosity (G) and the number of pores/area showed no correlation with porosity (H). Each dot represents the measurements in a given individual. The relationship between parameters was calculated using Pearson's correlation: * $p < 0.05$, ** $p < 0.01$, and *** $p < 0.001$. The curves represent the best-fitted lines for each parameter.

existing parent osteon. These pores most likely reflected the generation of new canals (Fig. 2). Pores were defined as type 2 pores when associated with a resorptive area that overlapped with the estimated position of earlier pores of existing parent osteons. These pores merely reflect the remodeling of existing canals (Fig. 2).

2. The position of type 2 pores in relation to their parent osteons in cortex (Fig. 2). Intra-osteonal type 2 pores (type 2_{IN} pores), when the pores resorption area was within the cement line of the existing parent osteon; cement-line breaking type 2 pores (type 2_{BK} pores), when the pores resorption area broke through the cement line of the existing parent osteon; and osteon coalescing type 2 pores (type 2_{CO} pores), when the pores resorption area overlapped with the pore of two or more existing parent osteons.
3. The remodeling stage of the pores. Based on their surface characteristics, all pores were further subtyped into 4 different categories according to their remodeling stage

(Fig. 3). Eroded pores (type E pores) had eroded surfaces, but no presence of osteoid surfaces; mixed eroded and formative pores (type EF pores) had both eroded and osteoid surfaces; formative pores (type F pores) had osteoid surfaces, but no eroded surfaces; while quiescent pores of osteons (type Q pores) had a terminated remodeling/formation and no signs of new erosions. Pores with remodeling stage E to F (E-F) are collectively referred to as pores with a non-terminated remodeling.

The pores diameters, areas, as well as their osteons diameters were measured. The pore and osteon diameter was measured as the diameter of the largest circle fitting within the pore, or its associated osteon. This diameter has been reported to correspond to the diameter of the largest ball than can be inflated within the pores and osteons cylindrical structures in three dimensions, even when they were oblique cut.⁽¹⁴⁾ Here it was critical that the observer detected the cement line of the most recent event at each remodeling site, and not the cement line from earlier events at the same site. Here, the mapping and

Histological appearance of eroded pores - new intracortical remodeling sites

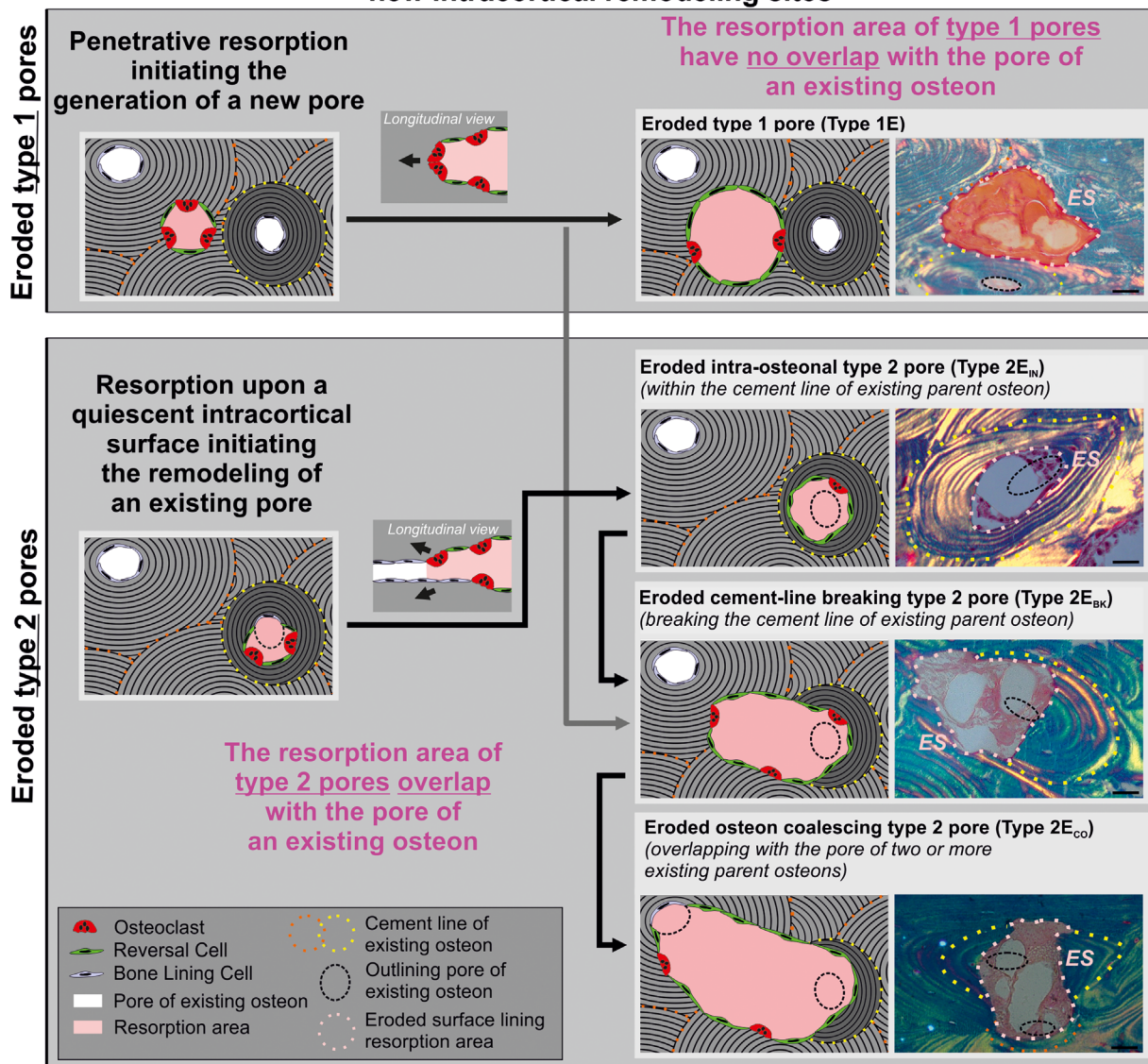


Fig. 2. Histological appearance and classification of eroded pores that reflect the reversal-resorption phase of new intracortical remodeling sites. The micrographs are from Masson's Trichrome stained section under polarized light. The eroded type 1 pores were classified as those having a resorption area that showed no overlap with pores of existing osteons, corresponding to new pores generated by penetrative resorption. Some of the pores originating from a penetrative resorption were classified as eroded cement-line breaking type 2 pores, as their resorption area expanded upon the pore of an existing osteon. The eroded type 2 pores were classified as those having a resorption area that overlapped with pore of an existing osteons, corresponding to the remodeling of an existing pore. The eroded type 2 pores that were within the cement line of the existing parent osteon were classified as eroded intra-osteonal type 2 pores. The eroded type 2 pores having a larger resorption area breaking the cement line of the existing parent osteon were classified as eroded cement-line breaking type 2 osteons, while those having an even later resorption that overlapped with the pore of two or more existing parent osteons were classified as eroded osteon coalescing type 2 pores. Scale bars = 25 μ m.

validation of the pores category and measurements by two observers was essential to prevent this potential mistake. The observers were not independent, as the second observer systematically reviewed the analysis conducted by the primary observer. Upon disagreement, the specific pore was discussed until consensus was reached. The completely sealed pores and their associated remodeling sites were also included in the analysis.⁽⁴¹⁾

Finally, the cortical tissue and pore areas were measured using a point grid, and subsequently used to calculate the cortical

porosity, thickness, and density of pores (number of pores per cortical area). The investigated sections were blinded prior to the analysis.

3D reconstruction

The 3D reconstructions of representative type 1 and type 2 pores were based on micrographs of 80 alternating Masson's trichrome-stained and osteopontin-immunostained consecutive

sections obtained from one iliac bone specimen. The 80 sections/micrographs represent 560 μm of the cortex along the axis of the intracortical canals. The micrographs were stacked, aligned and selected type 1 and 2 events/pores were converted into 3D structures of type 1 and 2 remodeled canals using Amira software version 5.4.1 (FEI, Hillsboro, OR, USA), as described.⁽⁴⁰⁾

Statistical analysis

Age and porosity associations of the mean percentage of the pore number or the porosity corresponding to given pore types in each of the 35 women were statistically compared using Pearson's correlation test (r_p) or Spearman's (r_s) correlations test. The statistical significance of the differences between the proportion of the different pore types and their contribution to the porosity and pore diameter was assessed using a Student's t test or a Mann-Whitney test when two types were compared, and a Kruskal-Wallis test followed by a Dunn's posttest when more than two types were compared. The D'Agostino and Pearson Omnibus normality test was used to address whether the percentages were normally distributed. The statistical analysis and graphs were all prepared in GraphPad Prism, version 6 (GraphPad Software Inc., La Jolla, CA, USA).

Results

The detailed histological investigation of the cortical bone of iliac bone specimens from 35 women included collectively 4095 pores/osteons. All the identified pores/osteons were mapped, as depicted in Fig. 1, and classified according to the characteristics of the associated remodeling site, as presented in Figs. 2 and 3. The identified 2D remodeling sites provided a cross-sectional status of the 3D intracortical remodeling events generating or remodeling the pores as they passed through the plane of the histological sections, and the respective pores contribution to the cortical porosity.

An increased pore diameter and not pore density associates with increased cortical porosity during aging

The investigated iliac bone specimens had a significant age-associated higher cortical porosity (Fig. 1C) and smaller cortical thickness (Fig. 1F). The higher cortical porosity with age seemed primarily to be the result of a larger pore diameter rather than a higher pore density, because only the mean pore diameter correlated positively with age and porosity (Fig. 1D, G), while the pore density (number of pores per area) showed no correlation with age or porosity (Fig. 1E, H).

Classification and diameter of pores according to their remodeling type, stage, and position

The investigation included all cross-sectional pores of the vascularized intracortical canal network composed of both Haversian and non-Haversian canals. A total of 4095 pores were investigated in the 35 iliac specimens, giving a mean of 117 pores per specimen (range, 63–179 pores). The pores were not classified according to whether they reflect Haversian or non-Haversian canals, but according to their remodeling type, stage, and position, as described in the Materials and Methods section and in Figs. 2 and 3.

The intracortical remodeling is initiated by a resorption phase, conducted by bone-resorbing osteoclasts, which is followed by a mixed reversal-resorption phase; where the eroded bone surface is colonized by mononucleated osteoblastic reversal cells intermixed with scattered osteoclasts, expanding the resorbed area. Intracortical pores reflecting new 2D remodeling sites in the initial resorption phase or subsequent the reversal-resorption phase are identified as eroded pores (type E pores) with new eroded surfaces. These eroded pores are either generated by a penetrative resorption, generating a new eroded pore (type 1E pore) having no overlap with the pore of an existing osteon, or by resorption within a quiescent intracortical surface, generating an eroded pore upon the pore of an existing osteon (type 2E pore) (Fig. 2).

The eroded type 2 pores were further categorized according to their resorption areas position relative to their parent osteons. The eroded type 2 pores having a small resorption area were often classified as eroded intra-osteonal type 2 pores (type 2E_{IN} pores), as they were within the cement line of the parent osteon (Fig. 2). The eroded type 2 pores having a larger resorption area that expanded beyond the cement line of the parent osteon was classified as eroded cement-line breaking type 2 pores (type 2E_{BK} pores) or as eroded osteon coalescing type 2 pores (type 2E_{CO} pores), if they expanded upon the pores of additional existing osteons (Fig. 2). Note that pores that originate from a penetrative resorption may also be classified as type 2E_{BK} or 2E_{CO} pores, if their resorption area had expanded upon the pores of existing osteons (Fig. 2).

As the eroded pores enter the formation phase, the pores first have both eroded and osteoid (formative) surfaces (type EF pores) and then eventually solely osteoid (formative) surfaces (type F pores) (Fig. 3). The pores with a terminated bone remodeling were classified as quiescent pores (type Q pores) (Fig. 3). In the formative and quiescent pores the remodeling type and position were defined based on their original resorption area, which were outlined by their osteons cement line (Fig. 3).

The diameter of the pores was highly variable and dependent on the pores classification (Fig. 4A). In general, type 2 pores had a significantly larger median diameter than type 1 pores. Within type 1 pores, type 1EF pores had the largest median diameter. Within type 2 pores, type 2E and 2EF pores had the largest median diameter, whereas type 2Q pores had the smallest median diameter. Moreover, type 2_{CO} pores had a significantly larger median diameter than type 2_{BK} pores, which then again had a significantly larger median diameter than type 2_{IN} pores. Of note, the enlarged type 2E_{CO} and 2EF_{CO} pores often had a very irregular shape (Fig. 4B, C). From a 3D perspective, type 2E_{CO} pores reflect enlarged eroded cavities, leading to the coalescence of multiple canals, which are interconnected with neighboring canals (Fig. 4D). This eroded cavity is much larger than the adjacent narrow canal corresponding to type 1Q pores (Fig. 4D).

Type 2 pores contribute more than type 1 pores to the age-induced cortical porosity

In the iliac bone specimens from 35 women, the majority of the pores were type 2 pores (Fig. 5A). The proportion of type 2 pores showed a significant positive correlation with the age of the women and the specimen's cortical porosity, while the

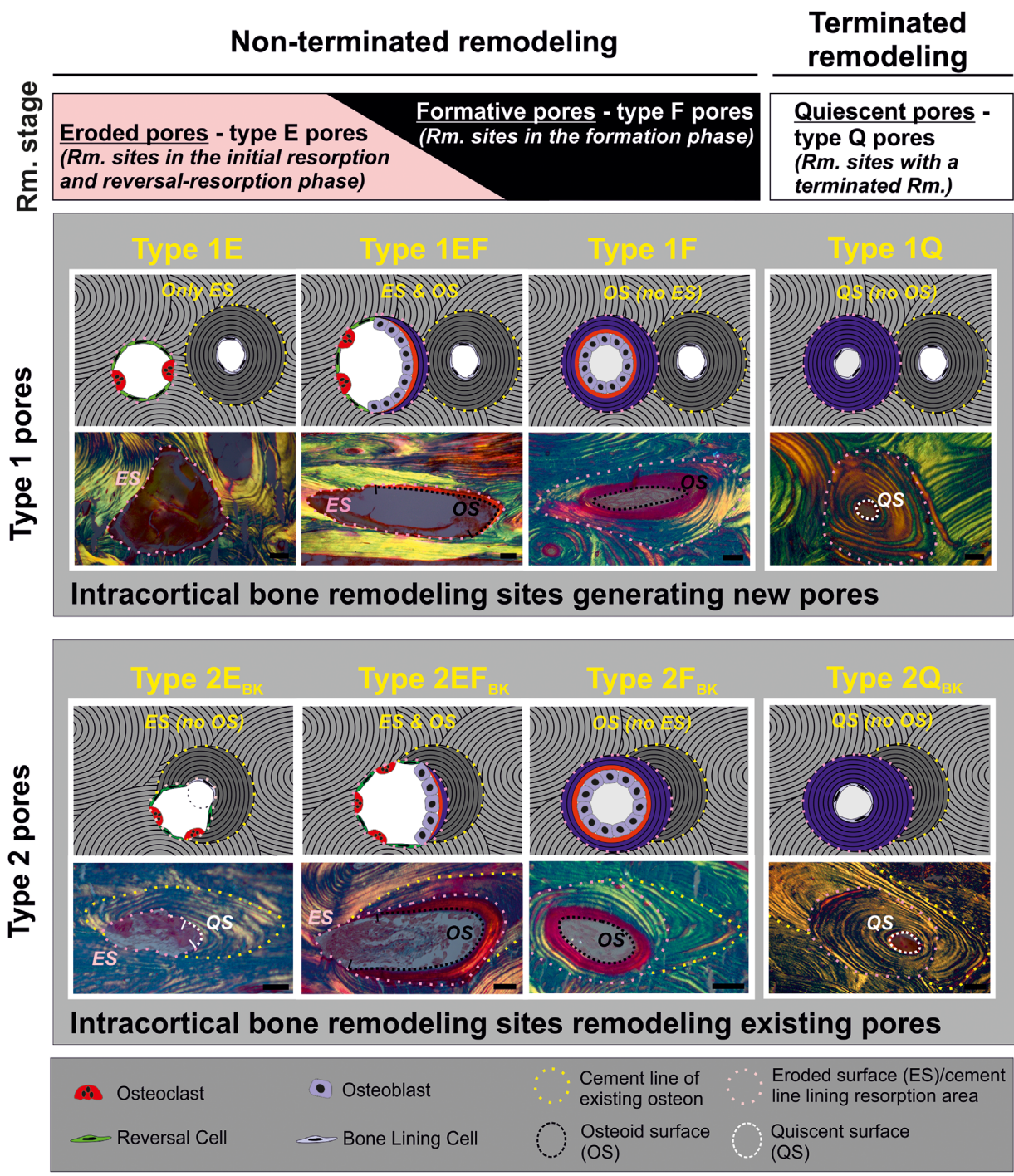


Fig. 3. Histological appearance and classification of pores reflecting remodeling sites that are at different remodeling stages. Both type 1 and type 2 pores were separated into four remodeling stages: E, EF, F, and Q. The illustrations show these different remodeling stages of type 1 pores and type 2_{BK} pores in Masson's trichrome stained sections under polarized light. The eroded pores with new eroded surfaces colonized with osteoclast and reversal cells reflect remodeling site in the reversal-resorption phase. The mixed eroded and formative pores with both eroded and osteoid surfaces reflect the transition from the reversal-resorption phase to the formation phase. The formative pores with osteoid surfaces colonized with osteoblasts reflect remodeling sites in the formation phase. The quiescent pores with quiescent surfaces colonized with bone lining cells reflect remodeling sites with a terminated remodeling. Note that the eroded surface is embedded as the cement line during the bone formation, and that the eroded surface and cement line upon which new bone is formed outline the resorption area. The pores with remodeling stage E-F are collectively referred to as pores with a non-terminated bone remodeling. Scale bars = 25 μm. E = eroded; EF = mixed eroded and formative; F = formative; Q = quiescent.

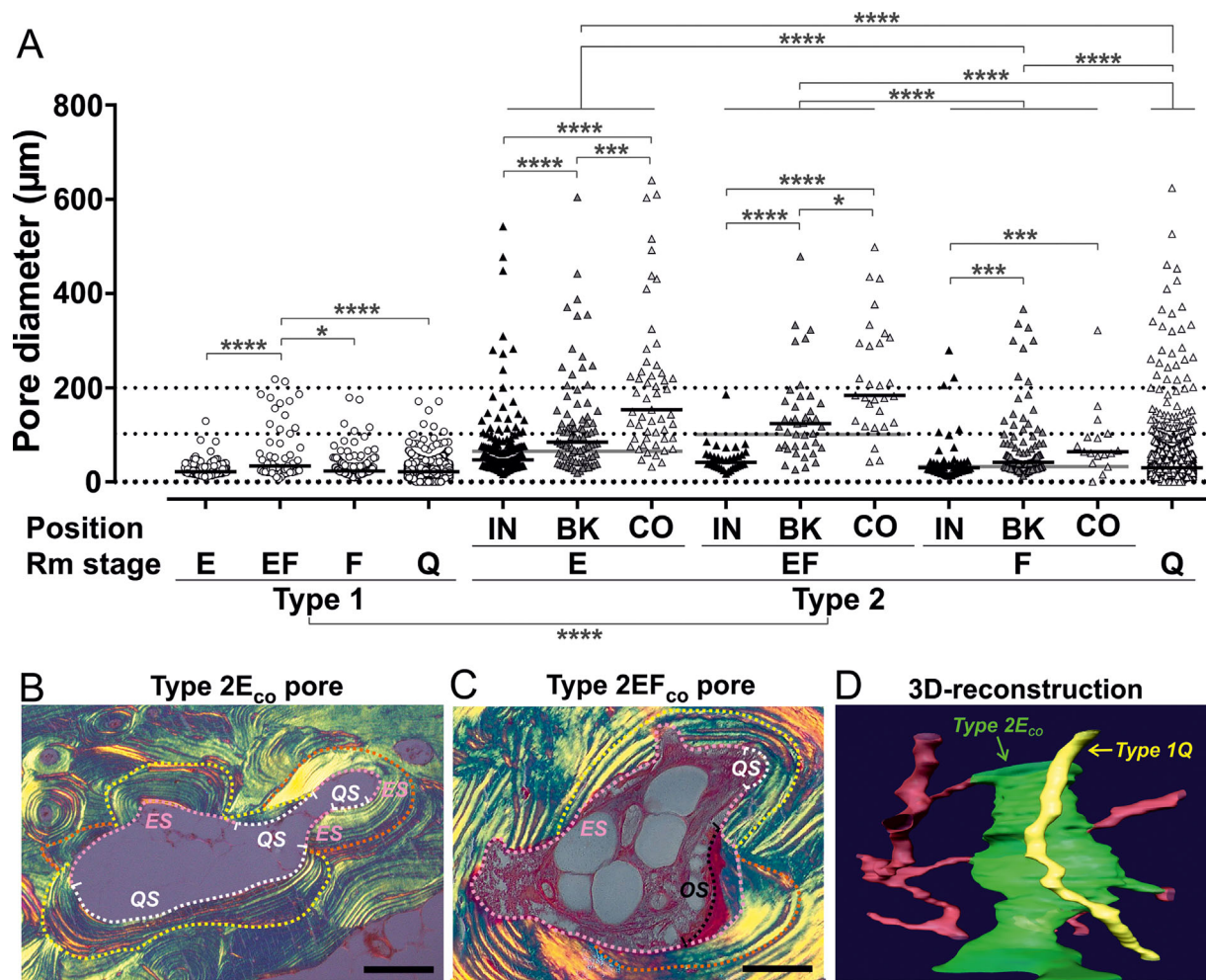


Fig. 4. Overall analysis of the different pore types individual diameters, and the histological and 3D appearance of the larger osteon coalescing type 2E and 2EF pores. (A) The diameter of the individual pore types classified according to the criteria shown in Figs. 2 and 3. Each dot represents the diameter of a given pore, and the black horizontal lines indicate the median for each classified type of pores, while the grey horizontal lines indicate the median for a group of pore types. The significant difference between the diameters of the respective pore types were calculated using a Mann-Whitney test (type 1 versus 2) or a Kruskal-Wallis test followed by a Dunn's posttest, when more than two groups were compared: * $p < 0.05$, *** $p < 0.01$, **** $p < 0.0001$. (B, C) Histological appearance of enlarged osteon coalescing type 2E and 2EF pores in Masson's Trichrome-stained sections under polarized light. As in Fig. 2, the resorption area is outlined by ES and QS, as well as the cement line below OS (white and pink dotted line). The cement lines of the existing osteons are outlined with yellow and orange dotted lines. Scale bars: 100 μm (B) and 50 μm (C). (D) 3D reconstruction of an eroded osteon coalescing type 2 pore based on 80 consecutive sections, showing that these 2D pores represent an enlarged 3D cavity in the cortex (green), which is much larger than the neighboring canal of quiescent type 1 pores (yellow). Note that the type 2E_{co} cavity connected to five intracortical canals (red). ES = eroded surfaces; QS = quiescent surfaces; OS = osteoid surfaces.

prevalence of type 1 pores showed a significant negative correlation with age and cortical porosity (Fig. 5B). Here the ratio between number of type 2 and type 1 pores (type 2/type 1 ratio) increased significantly with the age of the women and the specimen's cortical porosity (Supplementary Table 1). Type 2 pores appeared to reflect a larger proportion of the porosity than the proportion of pores, as the type 2 pores were larger than the type 1 pores (Fig. 5C). Accordingly, the type 2 pores contribution to the porosity showed a positive correlation with both age and porosity, whereas the contribution of type 1 pores showed a negative correlation with both age and porosity (Fig. 5D). A minor fraction of the investigated pores (median 1.3%) and their contribution to the porosity (median 2.2%) could not be categorized due to unclear lamellar structures or small folds in the sections (Fig. 5A, C).

Pores with a non-terminated remodeling contributes more than quiescent pores with a terminated remodeling to age-induced cortical porosity

Of the investigated pores, 77% were quiescent pores (type Q pores), having a terminated bone remodeling, while merely 23% were eroded to formative pores (type E-F pores), having a non-terminated remodeling (Fig. 5E). Considering the pores contribution to the porosity, type E-F pores contributed to 67% of the porosity (Fig. 5G), while their cumulative pore area reflected 5.4% of the cortical tissue area. The ratio between the number of type E-F pores and type Q pores showed no correlation with age, but a significant positive correlation ($p < 0.001$) with cortical porosity (Supplementary Table 1).

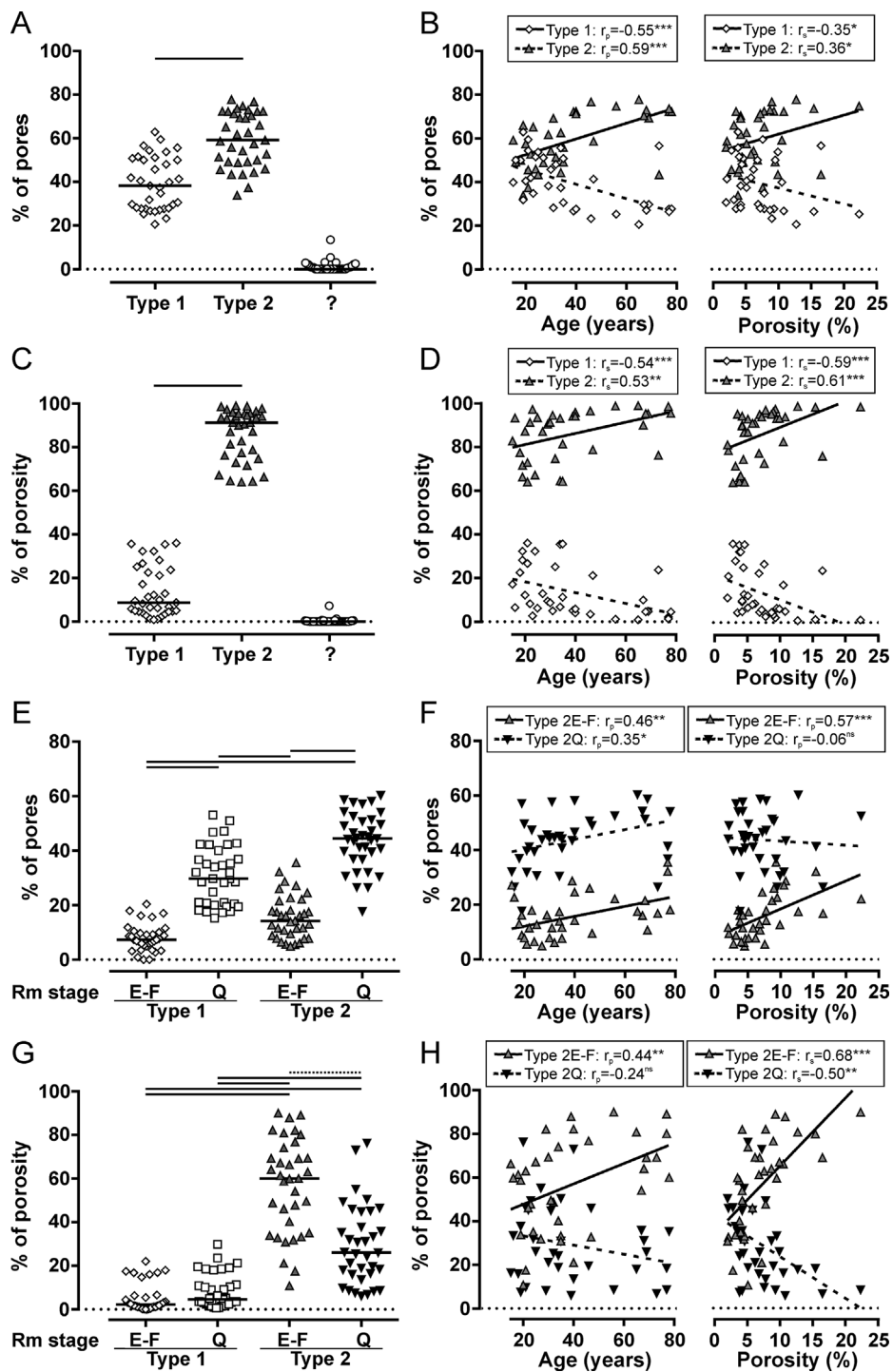


Fig. 5. Incidence of the pore types classified as shown in Figs. 2 and 3 and their contribution to the overall porosity in the iliac bone specimens of 35 women, as well as these parameters correlation with the women's age and the iliac specimens overall porosity. Each dot represents the measurements in a given specimen/women, the horizontal lines indicate the median for each type (A, C, E, G), and the curves in represent the best fitted-lines (B, D, F, H). (A–D) Type 1 versus type 2 pores. The type 2 pores were more prevalent (A) and contributed more to the pore area (C) than type 1 pores, and their prevalence (B) and pore area (D) was positively associated with age and porosity, while the prevalence (B) and pore area (D) of type 1 pores were negative associated with age and porosity. (E–H) Type E-F versus Q pores subdivided according to their remodeling type. The type Q pores were most prevalent (E), but the type 2E-F pores had the largest contribution to the pore area (G). Both the type 2E-F pores prevalence (F) and pore area (H) were positively associated with age and porosity. (A, C, E, F) Statistical significant differences between the incidence of pore types as well as their contribution to the overall porosity were calculated by a Student's *t* test (A), a Mann-Whitney test (C) and a Kruskal-Wallis test followed by a Dunn's posttest (E, F): dotted line, $p < 0.05$; line, $p < 0.001$. (B, D, E, F) The pore types prevalence and contribution to porosity association with age and porosity were calculated using a Spearman rank correlation test or a Pearson's correlation test: * $p < 0.05$, ** $p < 0.01$, *** $p < 0.001$.

In Fig. 5E–H, type E-F and Q pores were categorized into type 1 and 2 pores. The majority of both type 1 and 2 pores were type Q pores (Fig. 5E). The prevalence of both type 2Q and type 2E-F pores increased significantly with age, whereas only the prevalence of type 2E-F pores showed a positive correlation with cortical porosity (Fig. 5F). Considering the pores contribution to the cortical porosity, type 2E-F pores contributed significantly more to the porosity than type 1 and type 2Q pores (Fig. 5G). In fact, only type 2E-F pores showed a higher contribution to the porosity with age and a positive correlation with the overall cortical porosity, whereas type 2Q pores showed a negative correlation with porosity and unchanged with age (Fig. 5H).

Eroded type 2 pores contribute more than formative type 2 pores to age-induced cortical porosity

When subcategorizing type 2E-F pores according to their remodeling stage, 54% of these type 2E-F pores were eroded pores (type 2E pores), while 18% were mixed eroded and formative pores (type 2EF pores) and 28% were formative pores (type F pores) (Fig. 6A). This corresponded to a median ratio of 1.20 between the number of type 2E pores relative to the number of type EF and F pores (Supplementary Table 1). The prevalence of both type 2E and 2EF pores had a positive correlation with age and porosity, while the prevalence of type 2F pores remained unchanged (Fig. 6B). The ratio between type 2E pores over type 2EF and 2F pores was significant higher with age, but not correlated with cortical porosity (Supplementary Table 1). Similarly, a median ratio of 1.33 was obtained when not dividing the pores into type 1 and 2 pores. This ratio was also significantly positive correlated with age, but not correlated with cortical porosity (Supplementary Table 1).

When considering the contribution of type 2E-F pores to the porosity, type 2E pores reflected 74% of their contribution and 35% of the overall cortical porosity (Fig. 6C). Only the type 2E pores contribution to the porosity had a positive correlation with age and porosity. On the other hand, the contribution of type 2F pores had a negative correlation with age (Fig. 6D).

The generation of enlarged eroded osteon coalescing type 2 pores contributes significantly to age-induced cortical porosity

All type 2E pores were further subcategorized according to their resorption areas position relative to the existing parent osteons, as illustrated in Fig. 2. Most of the type 2E pores (62%) were eroded intra-osteonal type 2 pores (type 2E_{IN} pores), while 25% were eroded cement-line breaking type 2 pores (type 2E_{BR} pores) and 13% were classified as eroded osteon coalescing type 2 pores (type 2E_{CO} pores). The prevalence of the three positions of type 2E pores increased significantly with age and porosity with the exception of type 2E_{IN} pores, which was not correlated with cortical porosity (Fig. 6F).

Considering the different type 2E pores subcategories contribution to the cortical porosity, there were no significant difference between the different subcategories of type 2E pores contribution to the cortical porosity, as their contribution was highly variable between the different specimens (Fig. 6G). Here 49% of the type 2E pores contribution to the porosity reflected type 2E_{CO} pores (Fig. 6G). Only the type 2E_{CO} pores contribution to the cortical porosity had a positive correlation with age and cortical porosity, while the type 2E_{IN} and 2E_{BR} pores contribution had no correlation with age or porosity (Fig. 6H).

Discussion

Several studies have shown that during aging cortical bone becomes increasingly porous and thinner due to a dysfunctional intracortical bone remodeling. The present study establishes a novel classification of the pores contributing to cortical porosity, taking into consideration the characteristics of the associated remodeling sites. Owing to this classification, the study demonstrates that the accumulation of eroded pores upon pores of existing osteons (type 2E pores) is the main contributor to age-induced increase in the iliac cortical porosity. Moreover, these accumulating eroded type 2 pores expand their resorptive area, forming enlarged eroded osteon coalescing type 2 pores/cavities, which have a major contribution to the increased cortical porosity during aging in women, as summarized in Fig. 7 and discussed below.

Increased pore diameter, not density, contributes to increased cortical porosity with age

The present study first showed that iliac cortical bone from women had a higher cortical porosity together with lower cortical thickness with age, as previous shown in cortices from iliac,^(7,42) femur,^(43,44) and rib.^(45,46) Importantly, the increased cortical porosity, as well as the women's age, was associated with an increased pore diameter, and not associated with an increased pore density. This highlights that the age-induced increased cortical porosity in the investigated iliac specimens is the result of an increased pore size, not an increased pore density, which is in line with previous studies of the femur midshaft.^(43,44,47–49) Moreover, this supports that the overall age-induced changes in the cortical porosity in the iliac specimens resamples the age-induced changes reported in the femur midshaft.

Classification of the intracortical remodeling sites of pores contributing to cortical porosity

In order to investigate the intracortical remodeling sites generating the pores contributing to age-induced cortical porosity, we established the described classification of the intracortical pores and their associated remodeling site. The three criteria included in this classification is the outcome of a very comprehensive and detailed histological investigation of all 4095 pores in the 35 women and their associated intracortical remodeling sites within the investigated cortices. This was only possible because each pore was carefully mapped on a printed map of the cortex, making it possible to trace back the individual pores. The three classification criteria reported in this study link many of the selective criteria previously reported in the literature.^(10,30–34,36–39,50–52) Most importantly, the classification takes into account that the intracortical remodeling sites not only generate new pores (type 1 pores), but also remodel existing pores (type 2 pores),^(30–34,36,38,39) as well as the remodeling stage of the pores.^(12,14,52)

The classically depicted intracortical remodeling events,^(10,27) initiated by a penetrative cutting cone generating a new canal were in the cross-sections classified as type 1 pores. The eroded type 1 pores reflected these remodeling events that were in the recent reported reversal-resorption phase⁽¹¹⁾ when passing through the plane of the investigated histological cross section. The eroded type 1 pores had a resorption area that within the plane of the histological cross-sections had expanded upon the

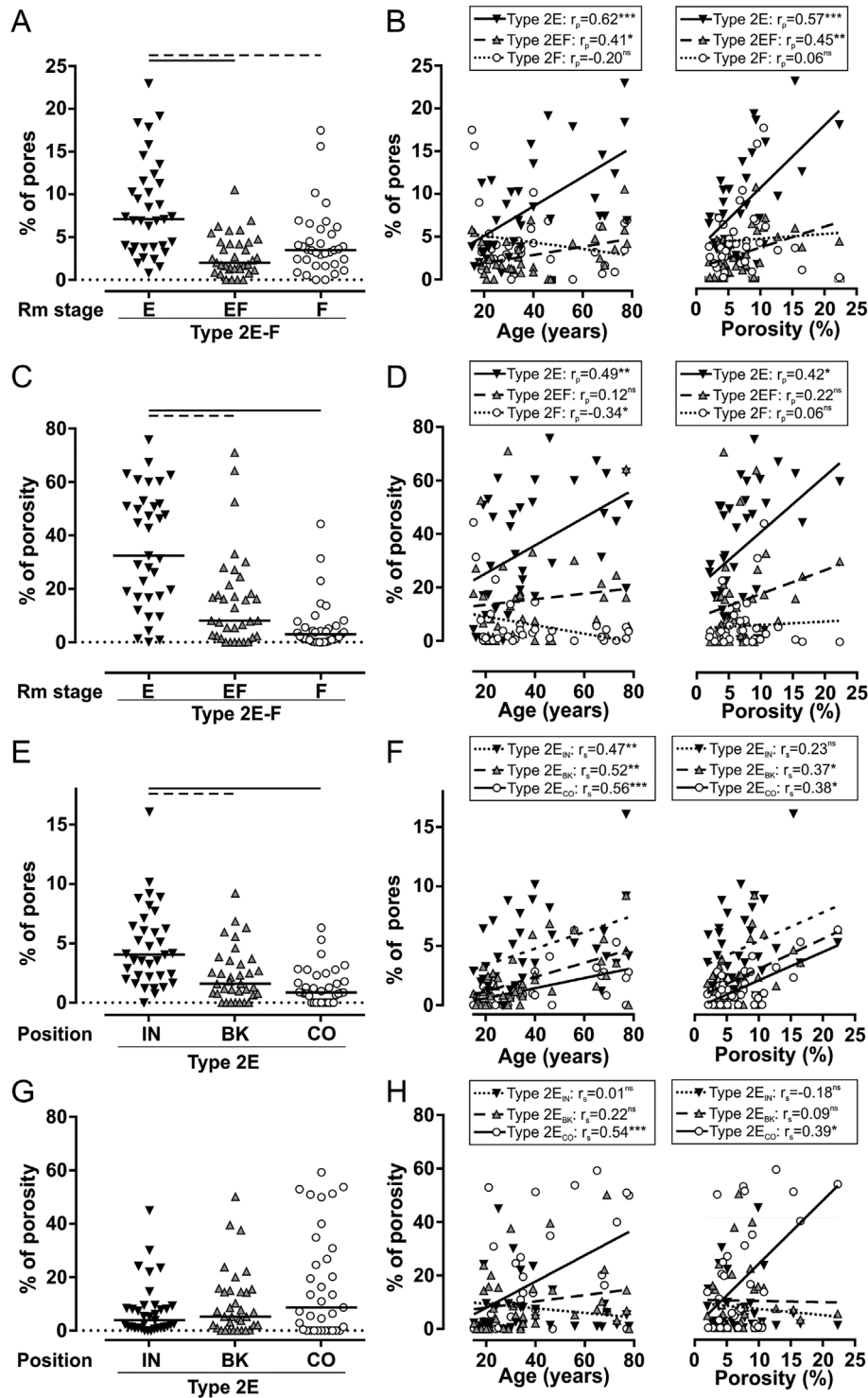


Fig. 6. Close-up on type 2E-F pores (A–D) and type 2E_{IN-CO} pores (E–H) prevalence, contribution to the overall porosity, and association with age and overall porosity. Each dot represents the measurements in a given individual, the horizontal lines indicate the median for each type (A, C), and the curves represent the best fitted-lines (B, D). (A–D) Type 2E pores were more prevalent (A) and had a larger contribution to the pore area (C) than type 2EF or 2F pores, and were positively associated with age and porosity (B, D). Note that type 2F pores contribution to the pore area has a negative correlation with age (D). (E–H) Type 2E_{IN} pores were more prevalent than type 2E_{BK} and type 2E_{CO} pores (E), but there was no difference between the different subgroups of type 2E pores contribution to the pore area (G). The prevalence of all positions of type 2E pores increased with age and porosity (F), but only the type 2E_{CO} pores contribution to the porosity increased with age and porosity (H). Statistical significances between the incidence of pore types as well as their contribution to the overall porosity were calculated using a Kruskal-Wallis test followed by a Dunn's posttest (C): hatched line, $p < 0.01$; line, $p < 0.001$. Age and porosity associations were assessed by Pearson's correlation: * $p < 0.05$, ** $p < 0.01$, *** $p < 0.001$.

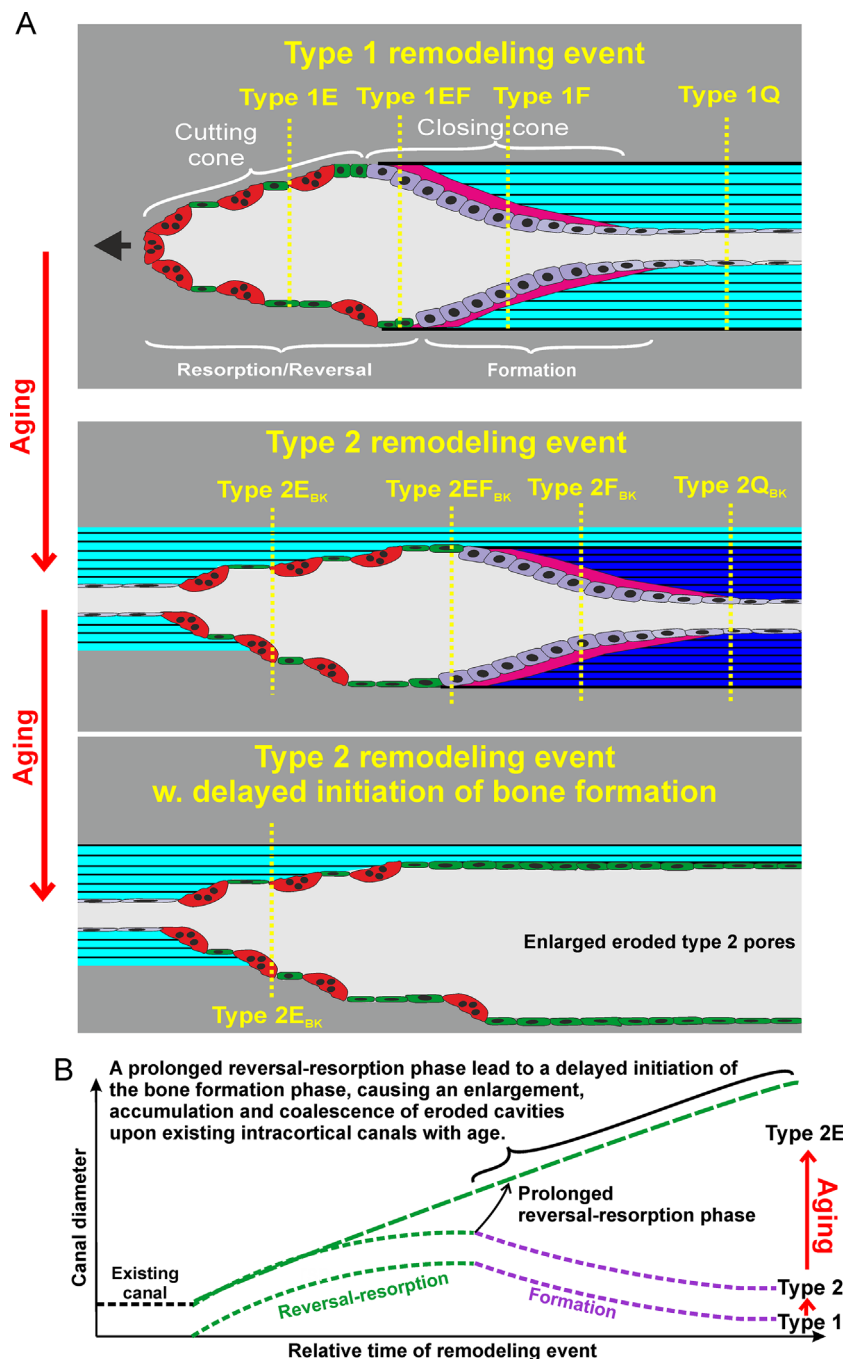


Fig. 7. Model illustrating that during aging the intracortical bone remodeling events are increasingly transformed into type 2 remodeling events, remodeling existing canals. Moreover, these events during aging more often have a non-terminated remodeling with a prolonged reversal-resorption phase relative to the formation phase. This may likely be the result of a delayed or absent initiation of bone formation in some of these type 2 events (A). This prolonged reversal-resorption phase causes an extended resorption, enlarging the cumulative eroded type 2 pores. This enlargement facilitates their coalescence into eroded osteon coalescing type 2 pores, which forms even larger cavities (B). (A) In the model osteoclasts are red, osteoprogenitor/reversal cells colonizing eroded surfaces are green, bone-forming osteoblasts colonizing osteoid surfaces are purple and turning grey as they transform into bone lining cells on quiescent surfaces, the osteoid is red and the respective bone structural units are light or dark blue.

pore of an existing osteon were classified as eroded cement-line breaking type 2 pores, even though they did not originate from erosion within an existing pore at this plane of the histological section. When the remodeling events generating a new canal entered the formation phase within the plane of the histological

section, they were classified as formative type 1 pores, and quiescent type 1 pores, when the remodeling was terminated. Although, 38% of the pores were identified as a type 1 pore they only contributed to 9% of the porosity, as they were in general smaller than the type 2 pores. The remodeling sites generating

type 1 pores identified in the present study are not directly comparable with the previous reported type 1 remodeling sites^(30,32,39) or single-zoned osteons,⁽³¹⁾ which seems to include the pores categorized as cement-line breaking or osteon coalescing type 2 pores.

The remodeling of existing pores was originally observed in human ribs by Jaworski and colleagues,⁽³⁰⁾ who reported the existence of small erosion widening an otherwise inactive old Haversian system. Similar small erosions have also been referred to as type II resorption cavities,⁽³²⁾ and reported to remain within the boundaries of the parent osteons, as the eroded intra-osteonal type 2 pores in the present study. When undergoing bone formation, these pores are characterized as formative intra-osteonal type 2 pores, reflecting the previous reported type II forming osteons.⁽³²⁾ When bone formation was terminated, these pores were characterized as quiescent intra-osteonal type 2 pores, which correspond to the previous reported new osteons in old osteons,^(30,33,35,51) double-zoned osteons,^(31,38) and type II osteons.^(32,36) Collectively, these intra-osteonal type 2 pores corresponded to 37% of the identified type 2 pores.

Importantly, the resorption area of the eroded type 2 pores may expand beyond the cement lines of the parent osteons, forming eroded cement-line breaking type 2 pores. The cement-line breaking type 2 pores corresponded to 51% of the type 2 pores and to 34% of the overall porosity. These cement-line breaking type 2 pores may likely reflect cross-sections of so-called "breakout zones."^(33,35,36) These breakout zones were described in 3D histological tracings of remodeling events in serial cross-sections of cortical bone from dogs, baboons, and humans,⁽³³⁾ as well as synchrotron radiation μ CT scans of human midshaft femur.^(35,36) Here the pores resampling the cement-line breaking type 2 pores were reported to reflect the graduate transition (breakout) from intra-osteonal type 2 pores to type 1 pores, and vice versa. Indeed, one may argue that all remodeling events observed as type 1 pores within the plane of the histological section from a 3D perspective must originate from events initiated on the surface of existing canals, or from events penetrating in from the endosteal or periosteal surface.⁽³⁶⁾

The resorption area of some eroded cement-line breaking type 2 pores expanded upon multiple pores of existing osteon, forming enlarged eroded osteon coalescing type 2 pores. These pores may potentially also originate from the coalescence of adjacent eroded cement-line breaking type 2 pores, as the pores with an active remodeling have been reported to occur in clusters.⁽⁵³⁾ Furthermore, these pores may, in part, reflect so-called composite osteons, which were reported to result from coalescence of multiple osteons.⁽⁵⁰⁾ Still, the composite osteons were originally described as formative and quiescent pores, and not as eroded pores.⁽⁵⁰⁾ Nevertheless, one may indeed argue that a great part of originally described quiescent composite osteons actually were coalescing due to new erosions, as the eroded osteon coalescing type 2 pores in this study. Here one should note the similarity between the eroded osteon coalescing type 2 pore illustrated in Fig. 4B and the quiescent composite osteon illustrated by Bell and colleagues.⁽⁵⁰⁾ Moreover, the composite osteons with formative surfaces may also still have a lot of eroded surfaces. Interestingly, the eroded and mixed eroded and formative osteon coalescing type 2 pores investigated in this study had the largest median diameter among the different categories of pores. This is again in line with the previous investigated composite osteons, which were

reported to reflect 83% of the so-called giant canals, having a diameter above 385 μ m, in the human femur neck.⁽⁵⁰⁾

Collectively, the categories included in the present study link many of the previous reported criteria and terminologies used to describe the pores and osteons. This provides a robust and integrated classification of the pores and osteons according to the associated intracortical remodeling sites, which pinpoints to the biological events generating the pores contributing to increased cortical porosity during aging.

Age-induced cortical porosity results mainly from the accumulation of eroded type 2 pores

Owing to this novel classification, the current study was able to stepwise pinpoint the remodeling type and stage of the pores having a major contribution to the age-induced increase in cortical porosity.

First, the study revealed that aging and the associated increased cortical porosity were strongly associated with a shift in the pores remodeling type from type 1 to type 2. Type 2 pores were in general larger than type 1 pores, and the type 2 pores did not reflect the generation of new pores, as the case for type 1 pores. Indeed, the generation of osteon coalescing type 2 pores, corresponding in part to the composite osteons⁽⁵⁰⁾; actually reduce the density of pores. Collectively, this may explain why the pore size increased and the density of pores was unchanged with age and porosity in the present study of iliac cortical bone and in previous studies of the femur midshaft.^(43,44,47-49) From a 3D perspective this implies that the intracortical remodeling events initiated on surfaces of existing canals with age to a less extent branch off and form new canals, observed as type 1 pores.^(35,36)

Second, the study revealed that those type 2 pores contributing the most to the cortical porosity with aging were preferentially pores with a non-terminated remodeling. This is in line with the notion that the intracortical bone turnover gradually increase with age and especially after menopause.^(12,19) Still, the quiescent type 1 and 2 pores having a terminated remodeling were more prevalent than those with a non-terminated remodeling, and the prevalence of quiescent type 2 pores had a positive correlation with age. On the contrary, these quiescent pores seemed only to have minor contribution to the porosity during aging. This negligible contribution of the quiescent pores with a terminated remodeling to the age-induced cortical porosity, questions the importance of the previous reported negative BMU balance between the extent of resorption and formation in these quiescent pores to the age-induced cortical porosity.^(12,14) Importantly, these studies did not consider that the remodeling may occur upon existing pores, meaning that they may have overestimated the quiescent pores most recent final resorption area; ie, osteon diameter. Future studies reassessing the extent of resorption, formation and the BMU balance between the two within the osteons of quiescent pores, taking into consideration the remodeling type, are therefore needed; in order to fully understand the effect of aging on the BMU balance and its contribution to age-induced cortical porosity.

Third, the study revealed that type 2 pores with a non-terminated remodeling cumulating during aging preferentially were eroded type 2 pores, corresponding to remodeling sites in the reversal-resorption phase. Importantly, the prevalence of formative type 2 pores was lower than the eroded type 2 pores and unchanged with age and porosity, while their contribution

to the porosity actually was lower with age. In other words, there were more eroded pores than formative pores, and the ratio between the two was actually higher with age, as previous reported.^(27,54) This ratio is greatly in conflict with the notion that the short initial resorption phase and longer mixed reversal-resorption phase roughly takes weeks and the formation phase takes months.⁽²⁷⁾ According to this notion, one should expect a ratio around 0.25 and not the ratio of 1.33 obtained in the current study. Assuming that the investigated cortices have a steady-state remodeling or only a gradual increase in bone turnover, it implies that the reversal-resorption phase in general takes longer time than the formation phase. On the other hand, it could also imply that the reversal-resorption phase is extensively prolonged at given remodeling sites, while other may still have a much shorter “normal” reversal-resorption phase. As the reversal-resorption phase ends when the bone formation is initiated, the prolonged reversal-resorption phase must be directly linked with a delayed initiation of the subsequent bone formation, which recently was reported to be controlled by the recruitment rate of osteoprogenitor cells during the reversal-resorption phase.⁽¹¹⁾ A direct example of an intracortical remodeling event with a prolonged reversal-resorption phase was previously reported by Tappen,⁽³³⁾ who traced intracortical canals in serial cross-sections of a human rib. One of these canals was covered with eroded surfaces throughout the entire sequence of 3000 μm , while only a short sequence of 300 μm had signs of bone formation on one wall. In cancellous bone, a similar accumulation of eroded surfaces reflecting a prolonged reversal-resorption phase has been reported to contribute to the bone loss in elderly, as well as in osteoporotic patients and animal models.^(20–22,24–26,55,56)

Eroded type 2 pores coalesce into enlarged eroded cavities with age

Owing to the classification, the present study was able to show that aging and the related increased cortical porosity was associated with the generation of eroded osteon coalescing type 2 pores, forming enlarged 3D cavities within the cortex. Even though these eroded osteon coalescing type 2 cavities represented only a small percentage of the total number of pores, they had a major contribution to the overall porosity, especially in the investigated elderly women. The enlarged resorption area of these cavities may likely be the result of a prolonged reversal-resorption phase, which was recently linked to an extended radial resorption.⁽¹¹⁾ Moreover, these cavities may, in part, reflect the giant canals/pores with a diameter above 385 μm described by Bell and colleagues,⁽³⁷⁾ whose prevalence increased with age in the femur midshaft of both men and women, and which were more prevalent in the anterior part of the femur neck cortex of female fracture patients compared to controls.^(57,58) The enlarged eroded osteon coalescing type 2 cavities may also, in part, reflect the enlarged, coalescing and irregular shaped pores illustrated in the endosteal part of femoral cortex of elderly.⁽⁵⁹⁾ Indeed, the latter pores may originate from or directly reflect eroded osteon coalescing type 2 cavities reported in the current study, highlighting that these latter pores may be the result of a prolonged reversal-resorption phase due to a delayed or absent initiation of bone formation.⁽¹¹⁾

Limitations of the study

A limitation of the present study was the age distribution of the women from which the iliac bone specimens were

obtained and the number of specimens included. Here especially the limited number of samples from women aged 40 to 60 years made it impossible to address whether menopause had any additive effect that were independent of the women’s age, which accordingly was not within the scope of this study. Moreover, additional samples may have improved the significance of the correlations, but it is unlikely that the inclusion of additional samples would affect the main conclusions drawn in this study. In addition, one needs to validate whether the age-induced cortical porosity varies between different skeletal sites and between the genders, or whether the findings of the current study are representative for all skeletal sites and both genders. Future studies are warranted to address the variability in the age-induced cortical porosity between skeletal sites and genders, as well as the effect of menopause in women using the pore classification established in the present study.

Conclusion

Collectively, the present study shows that age-induced cortical porosity reflects an increased pore size rather than increased pore density in iliac cortical bone in women. Furthermore, the study establishes a novel classification of the intracortical pores used to investigate their generation and modulation, which is designed to identify the critical intracortical remodeling events responsible for age-induced cortical porosity. Owing to this classification, the study demonstrates that the age-induced cortical porosity in the investigated iliac specimen is mainly the results from cumulative eroded pores that originate by erosion upon existing canals (type 2 pores) and coalesce into enlarged cavities. Here, the cumulative eroded pores reflect that the reversal-resorption phase of the intracortical remodeling events is in general prolonged, leading to a delayed or absent initiation of bone formation.⁽¹¹⁾ In a wider perspective, these results support the notion that the transition from the reversal-resorption phase to the formation phase is a critical step in physiological bone remodeling, and that its absence is a major contributor to bone loss during aging and osteoporosis.

Disclosures

All authors state that they have no conflicts of interest.

Acknowledgments

This work was supported by The Velux Foundation (VE-LUX34368) and the Danish Southern Region Research Grant (15/24851). We thank Birgit MacDonald and Kaja Søndergaard Laursen for their outstanding technical assistance, Dorie Birkenhäger-Frenkel and Alex Nigg from the Department of Pathology at Erasmus MC for collecting the bone specimens.⁽⁶⁰⁾

Author’ roles: The study was designed by CMA and TLA. The ethical approval and data handling related to the bone specimens was conducted by BE and JL. The analysis was conducted by CMA and TLA, whom also take the responsibility for the integrity of the data analysis. The data was analyzed by TLA and interpreted by CMA, JMD and TLA. The manuscript was drafted by CMA and TLA, and revised by all authors, whom also approved the final version.

References

1. Havers C. *Osteologia nova, or some new observations of the bones*. London: Smith; 1691. Available from: <https://archive.org/details/osteologianovaor00have>.
2. Leeuwenhoeck A. Microscopical observations of the structure of teeth and other bones: made and communicated, in a letter by Mr. Antohony Leeuwenhoeck. *Philos Trans R Soc Lond*. 1677;12:1002–3. Available from: <http://rstl.royalsocietypublishing.org/content/12/140/1002.extract>. DOI:10.1098/rstl.1677.0052.
3. Hattner R, Epker BN, Frost HM. Suggested sequential mode of control of changes in cell behaviour in adult bone remodelling. *Nature*. 1965;206(983):489–90.
4. Epker BN, Frost HM. A histological study of remodeling at the periosteal, haversian canal, cortical endosteal, and trabecular endosteal surfaces in human rib. *Anat Rec*. 1965;152(2):129–35.
5. Seeman E. Pathogenesis of bone fragility in women and men. *Lancet*. 2002;359(9320):1841–50.
6. Hansen S, Shanbhogue V, Folkestad L, Nielsen MM, Brixen K. Bone microarchitecture and estimated strength in 499 adult Danish women and men: a cross-sectional, population-based high-resolution peripheral quantitative computed tomographic study on peak bone structure. *Calcif Tissue Int*. 2014;94(3):269–81.
7. Bach-Gansmo FL, Bruel A, Jensen MV, Ebbesen EN, Birkedal H, Thomsen JS. Osteocyte lacunar properties and cortical microstructure in human iliac crest as a function of age and sex. *Bone*. 2016;91:11–9.
8. Frost HM. The skeletal intermediary organization. *Metab Bone Dis Relat Res*. 1983;4(5):281–90.
9. Parfitt AM. Osteonal and hemi-osteonal remodeling: the spatial and temporal framework for signal traffic in adult human bone. *J Cell Biochem*. 1994;55(3):273–86.
10. Johnson LC. Morphological analysis of pathology. In: Frost HM, editor. *Bone biodynamics*. Boston: Little, Brown; 1964. p. 543–654.
11. Lassen NE, Andersen TL, Pløen GG, et al. Coupling of bone resorption and formation in real time: new knowledge gained from human Haversian BMUs. *J Bone Miner Res*. 2017;32(7):1395–405.
12. Brockstedt H, Kassem M, Eriksen EF, Mosekilde L, Melsen F. Age- and sex-related changes in iliac cortical bone mass and remodeling. *Bone*. 1993;14(4):681–91.
13. Vedi S, Tighe JR, Compston JE. Measurement of total resorption surface in iliac crest trabecular bone in man. *Metab Bone Dis Relat Res*. 1984;5(6):275–80.
14. Broulik P, Kragstrup J, Mosekilde L, Melsen F. Osteon cross-sectional size in the iliac crest: variation in normals and patients with osteoporosis, hyperparathyroidism, acromegaly, hypothyroidism and treated epilepsy. *Acta Pathol Microbiol Immunol Scand A*. 1982;90(5):339–44.
15. Eriksen EF, Hodgson SF, Eastell R, Cedel SL, O'Fallon WM, Riggs BL. Cancellous bone remodeling in type I (postmenopausal) osteoporosis: quantitative assessment of rates of formation, resorption, and bone loss at tissue and cellular levels. *J Bone Miner Res*. 1990;5(4):311–9.
16. Eriksen EF, Gundersen HJ, Melsen F, Mosekilde L. Reconstruction of the formative site in iliac trabecular bone in 20 normal individuals employing a kinetic model for matrix and mineral apposition. *Metab Bone Dis Relat Res*. 1984;5(5):243–52.
17. Kragstrup J, Melsen F, Mosekilde L. Thickness of lamellae in normal human iliac trabecular bone. *Metab Bone Dis Relat Res*. 1983;4(5):291–5.
18. Lips P, Courpron P, Meunier PJ. Mean wall thickness of trabecular bone packets in the human iliac crest: changes with age. *Calcif Tissue Res*. 1978;26(1):13–7.
19. Seeman E. Age- and menopause-related bone loss compromise cortical and trabecular microstructure. *J Gerontol A Biol Sci Med Sci*. 2013;68(10):1218–25.
20. Andersen TL, Abdelgawad ME, Kristensen HB, et al. Understanding coupling between bone resorption and formation: are reversal cells the missing link? *Am J Pathol*. 2013;183(1):235–46.
21. Andreassen CM, Ding M, Overgaard S, Bollen P, Andersen TL. A reversal phase arrest uncoupling the bone formation and resorption contributes to the bone loss in glucocorticoid treated ovariectomised aged sheep. *Bone*. 2015;75C:32–9.
22. Jensen PR, Andersen TL, Hauge EM, Bollerslev J, Delaisse JM. A joined role of canopy and reversal cells in bone remodeling – Lessons from glucocorticoid-induced osteoporosis. *Bone*. 2015;73:16–23.
23. Andersen TL, Hauge EM, Rolighed L, Bollerslev J, Kjaergaard-Andersen P, Delaisse JM. Correlation between absence of bone-remodeling compartment canopies, reversal-phase arrest, and deficient bone formation in post-menopausal osteoporosis. *Am J Pathol*. 2014;184(4):1142–51.
24. Delaisse JM. The reversal phase of the bone-remodeling cycle: cellular prerequisites for coupling resorption and formation. *Bonekey Rep*. 2014;3:561.
25. Makris GP, Saffar JL. Disturbances in bone remodeling during the progress of hamster periodontitis. A morphological and quantitative study. *J Periodontal Res*. 1985;20(4):411–20.
26. Baron R, Magee S, Silverglate A, Broadus A, Lang R. Estimation of trabecular bone resorption by histomorphometry: evidence for a prolonged reversal phase with normal resorption in postmenopausal osteoporosis and coupled increased resorption in primary hyperparathyroidism. In: Frame B, Petts JT, editors. *Clinical disorders of bone and mineral metabolism*. 4th ed. Amsterdam: Excerpta Medica; 1983. p. 191–5.
27. Parfitt AM. The physiologic and clinical significance of bone histomorphometric data. In: Recker R, editor. *Bone histomorphometry: techniques and interpretation*. Boca Raton, FL: CRC Press; 1983. p. 144–222.
28. Kragstrup J, Melsen F, Mosekilde L. Thickness of bone formed at remodeling sites in normal human iliac trabecular bone: variations with age and sex. *Metab Bone Dis Relat Res*. 1983;5(1):17–21.
29. Riggs BL, Parfitt AM. Drugs used to treat osteoporosis: the critical need for a uniform nomenclature based on their action on bone remodeling. *J Bone Miner Res*. 2005;20(2):177–84.
30. Jaworski ZF, Meunier P, Frost HM. Observations on two types of resorption cavities in human lamellar cortical bone. *Clin Orthop Relat Res*. 1972;83:279–85.
31. Pankovich AM, Simmons DJ, Kulkarni VV. Zonal osteons in cortical bone. *Clin Orthop Relat Res*. 1974(100):356–63.
32. Richman EA, Ortner DJ, Schulter-Ellis FP. Differences in intra-cortical bone remodeling in three aboriginal American populations: possible dietary factors. *Calcif Tissue Int*. 1979;28(3):209–14.
33. Tappen NC. Three-dimensional studies on resorption spaces and developing osteons. *Am J Anat*. 1977;149(3):301–17.
34. Parfitt AM, Mathews CH, Villanueva AR, Kleerekoper M, Frame B, Rao DS. Relationships between surface, volume, and thickness of iliac trabecular bone in aging and in osteoporosis. Implications for the microanatomic and cellular mechanisms of bone loss. *J Clin Invest*. 1983;72(4):1396–409.
35. Arhatari BD, Cooper DM, Thomas CD, Clement JG, Peele AG. Imaging the 3D structure of secondary osteons in human cortical bone using phase-retrieval tomography. *Phys Med Biol*. 2011;56(16):5265–74.
36. Maggiano IS, Maggiano CM, Clement JG, Thomas CD, Carter Y, Cooper DM. Three-dimensional reconstruction of Haversian systems in human cortical bone using synchrotron radiation-based micro-CT: morphology and quantification of branching and transverse connections across age. *J Anat*. 2016;228(5):719–32.
37. Bell KL, Loveridge N, Reeve J, Thomas CD, Feik SA, Clement JG. Super-osteons (remodeling clusters) in the cortex of the femoral shaft: influence of age and gender. *Anat Rec*. 2001;264(4):378–86.
38. Nyssen-Behets C, Duchesne PY, Dhem A. Structural changes with aging in cortical bone of the human tibia. *Gerontology*. 1997;43(6):316–25.
39. Ortner DJ. Aging effects on osteon remodeling. *Calcif Tissue Res*. 1975;18(1):27–36.

40. Andersen TL, Sondergaard TE, Skorzynska KE, et al. A physical mechanism for coupling bone resorption and formation in adult human bone. *Am J Pathol.* 2009;174(1):239–47.
41. Andreasen CM, Delaisse JM, van der Eerden BCJ, et al. The balance between bone resorption and formation during intracortical osteonal bone remodeling: a study of transiliac bone biopsies from women. *J Bone Miner Res.* 2016; 31 Suppl 1. [Poster session presented at: Annual Meeting American Society for Bone and Mineral Research (ASBMR); 2016 Sep 16–19; Atlanta, GA, USA; Poster Sessions, Presentation Number: MO0257]. Available from: <http://www.asbmr.org/education/AbstractDetail?aid=99209603-5d86-43bf-8789-92759a2ea9c5>.
42. Parfitt AM. Age-related structural changes in trabecular and cortical bone: cellular mechanisms and biomechanical consequences. *Calcif Tissue Int.* 1984;36 Suppl 1:S123–8.
43. Thompson DD. Age changes in bone mineralization, cortical thickness, and haversian canal area. *Calcif Tissue Int.* 1980; 31(1):5–11.
44. Bousson V, Meunier A, Bergot C, et al. Distribution of intracortical porosity in human midfemoral cortex by age and gender. *J Bone Miner Res.* 2001;16(7):1308–17.
45. Sedlin ED, Frost HM, Villanueva AR. Variations in cross-section area of rib cortex with age. *J Gerontol.* 1963;18:9–13.
46. Barer M, Jowsey J. Bone formation and resorption in normal human rib. A study of persons from 11 to 88 years of age. *Clin Orthop Relat Res.* 1967;52:241–7.
47. Stein MS, Feik SA, Thomas CD, Clement JG, Wark JD. An automated analysis of intracortical porosity in human femoral bone across age. *J Bone Miner Res.* 1999;14(4):624–32.
48. Thomas CD, Feik SA, Clement JG. Increase in pore area, and not pore density, is the main determinant in the development of porosity in human cortical bone. *J Anat.* 2006;209(2):219–30.
49. Lerebours C, Thomas CD, Clement JG, Buenzli PR, Pivonka P. The relationship between porosity and specific surface in human cortical bone is subject specific. *Bone.* 2015;72:109–17.
50. Bell KL, Loveridge N, Jordan GR, Power J, Constant CR, Reeve J. A novel mechanism for induction of increased cortical porosity in cases of intracapsular hip fracture. *Bone.* 2000;27(2):297–304.
51. Morgan JTJaCd. Observations on the structure and Development of bone. *Philos Trans R Soc Lond.* 1853;143:109–39. Available from: <http://rstl.royalsocietypublishing.org/content/143/109.extract>. DOI:10.1098/rstl.1853.0004.
52. Agerbaek MO, Eriksen EF, Kragstrup J, Mosekilde L, Melsen F. A reconstruction of the remodelling cycle in normal human cortical iliac bone. *Bone Miner.* 1991;12(2):101–12.
53. Jordan GR, Loveridge N, Bell KL, Power J, Rushton N, Reeve J. Spatial clustering of remodeling osteons in the femoral neck cortex: a cause of weakness in hip fracture? *Bone.* 2000;26(3):305–13.
54. Jowsey J. Age changes in human bone. *Clin Orthop.* 1960;17:210–8.
55. Mosekilde L. Consequences of the remodelling process for vertebral trabecular bone structure: a scanning electron microscopy study (uncoupling of unloaded structures). *Bone Miner.* 1990;10(1):13–35.
56. Croucher PI, Garrahan NJ, Mellish RW, Compston JE. Age-related changes in resorption cavity characteristics in human trabecular bone. *Osteoporos Int.* 1991;1(4):257–61.
57. Bell KL, Loveridge N, Power J, Garrahan N, Meggitt BF, Reeve J. Regional differences in cortical porosity in the fractured femoral neck. *Bone.* 1999;24(1):57–64.
58. Bell KL, Loveridge N, Power J, Rushton N, Reeve J. Intracapsular hip fracture: increased cortical remodeling in the thinned and porous anterior region of the femoral neck. *Osteoporos Int.* 1999;10(3):248–57.
59. Zebaze RM, Ghasem-Zadeh A, Bohte A, et al. Intracortical remodelling and porosity in the distal radius and post-mortem femurs of women: a cross-sectional study. *Lancet.* 2010; 375(9727):1729–36.
60. Birkenhager-Frenkel DH, Courpron P, Hupscher EA, et al. Age-related changes in cancellous bone structure. A two-dimensional study in the transiliac and iliac crest biopsy sites. *Bone Miner.* 1988; 4(2):197–216.